Silva, G., & Drinkwater, B. (2018). Acoustic radiation force exerted on a small spheroidal rigid particle by a beam of arbitrary wavefront: Examples of traveling and standing plane waves. *Journal of the Acoustical Society of America*, *144*(5), [EL453]. https://doi.org/10.1121/1.5080529

Acoustic radiation force exerted on a small spheroidal rigid particle by a beam of arbitrary wavefront: Examples of traveling and standing plane waves

Glauber T. Silva[1, a)] **and Bruce W. Drinkwater**[2]

[1)] *Physical Acoustics Group, Instituto de Física, Universidade Federal de Alagoas, Maceió, AL 57072-970, Brazil*

[2)] *Department of Mechanical Engineering, University of Bristol, Bristol, BS8 1TR, United Kingdom*

glauber@pq.cnpq.br,

b.drinkwater@bristol.ac.uk

Abstract: We present the analytical solution of the acoustic radiation force exerted by a beam of arbitrary shape on a small spheroidal rigid particle suspended in an ideal fluid. We consider the long-wavelength approximation in which the particle is much smaller than the wavelength. Based on this theoretical development, we derive closed-form expressions for the radiation force of a traveling and standing plane wave on a prolate spheroidal particle in the dipole approximation. As validation, we recover the previous analytical result considering a standing wave interacting with a spheroid in axisymmetric configuration, as well as numerical results obtained with the boundary-element method.

[a)] Author to whom correspondence should be addressed.

1. Introduction

Nonspherical cells and microorganisms are routinely investigated in biological assays performed in acoustofluidic and acoustical tweezer devices. Some examples which significantly deviate from spherical shape include rod-like bacteria and biconcave red blood cells. In these acoustical devices, translational manipulation of small particles, which are much smaller than the wavelength, is performed employing the acoustic radiation force caused by ultrasonic waves.[1]

Most theoretical analyses of the acoustic radiation force in fluids assume that the particles have spherical shape.[2–11] More structured objects such as core-shell spherical particles have also been considered.[12] Besides, the secondary radiation force developed between two or more spherical particles has been analyzed.[13] All these studies are based on the partial-wave expansion of the incident and scattered waves in spherical coordinates. Analytical expressions of the radiation force are derived concerning the incident and scattering expansion coefficients. For a small particle, it need mean only the monopole and dipole scattering coefficients, i.e., the so-called dipole approximation, which are calculated from the boundary conditions on the particle surface. Moreover, the orthogonality of spherical wavefunctions used in the expansion are employed to decouple each mode and obtain a system of linear equations involving the expansion coefficients. However, when considering a nonspherical object, the boundary conditions formulated in spherical coordinates are no longer trivial. This happens because the radial distance to a particle surface point depends on the coordi-

nate angles. Consequently, the spherical wavefunctions are not necessarily orthogonal, which renders closed-form exact solutions of the radiation force be difficult to be attained.

The acoustic radiation force exerted on a rigid spheroidal particle by a standing wave was derived by Marston *et al.*[14] This result relies on the solution of the acoustic scattering by a spheroid in the long-wavelength limit.[15] However, it is limited to axisymmetric particles with respect to the incident wave. Aside from Marston's analytical result, seminumerical techniques that combine partial-wave spherical expansion and quadrature methods have been used to compute an approximate solution.[16] Additionally, numerical techniques such as boundary- and finite-element methods were also employed to calculate the radiation force.[17–19]

In this paper, we derive an analytical solution of the acoustic radiation force on a spheroidal particle with an arbitrary spatial orientation in the dipole approximation. The method is valid for an incident beam of an arbitrary wavefront. In so doing, we first recognize that the incident and scattered partial-wave expansions in spheroidal coordinates asymptotically match expansions in spherical coordinates at the farfield. Hence, the radiation force is calculated through the farfield method in which the radiation stress is integrated on a farfield control surface of spherical shape.[20] A closed-form expression is obtained for the force on a rigid prolate spheroid generated by a traveling and standing plane wave. In comparison with the case of a spherical particle of the same volume as the spheroid, the maximum radiation force deviation are 1/3 and 1/5 for, respectively, the traveling and standing plane wave.

Additionally, our theoretical prediction are in excellent agreement the numerical solution obtained with the boundary-element method given in Ref. 19.

2. Scattering theory

Consider an arbitrary acoustic wave of angular frequency ω and wavelength λ propagating in a nonviscous fluid of density ρ_0 and adiabatic speed of sound c_0. The wave is scattered by a prolate spheroidal particle with major and minor axis denoted by $2a$ and $2b$, respectively, as depicted in Fig. 1.a. The particle eccentricity is defined by $\varepsilon_0 = \sqrt{1-(b/a)^2}$. The coordinate system is set to the geometric center of the particle with the z-axis coinciding to the particle rotation axis. The particle defines a prolate spheroidal coordinate system through the transformations

$$x = \frac{d}{2}\sqrt{(\xi^2-1)(1-\eta^2)}\cos\varphi, \quad y = \frac{d}{2}\sqrt{(\xi^2-1)(1-\eta^2)}\sin\varphi, \quad z = \frac{d\xi\eta}{2}, \tag{1}$$

where d is the interfocal distance, $\xi \geq 1$ is the spheroidal radial coordinate, $-1 \leq \eta \leq 1$, and $0 \leq \varphi \leq 2\pi$ (see Fig. 1.b). The particle surface is determined by $\xi = \xi_0 = \varepsilon_0^{-1} = 2a/d$, while its volume is $V = 4\pi(d/2)^3\xi_0(\xi_0^2-1)/3$. A spherical particle is recovered by setting $\varepsilon_0 = 0$. The connection between the spheroidal coordinates with radial distance r and polar angle θ are

$$r = \frac{d}{2}\sqrt{\xi^2+\eta^2-1}, \quad \cos\theta = \frac{\eta\xi}{\sqrt{\xi^2+\eta^2-1}}. \tag{2}$$

The velocity potential function of the incident beam and scattered waves can be expressed by[21]

$$\phi_{\text{in}} = \phi_0 \sum_{n,m} a_{nm} S_{nm}(\epsilon, \eta) R^{(1)}_{nm}(\epsilon, \xi) \mathrm{e}^{\mathrm{i}m\varphi}, \tag{3a}$$

$$\phi_{\text{sc}} = \phi_0 \sum_{n,m} a_{nm} s_{nm} S_{nm}(\epsilon, \eta) R^{(3)}_{nm}(\epsilon, \xi) \mathrm{e}^{\mathrm{i}m\varphi}, \tag{3b}$$

where ϕ_0 is a constant, $\sum_{n,m} = \sum_{n=0}^{\infty} \sum_{m=-n}^{n}$, S_{nm} is the angular function of the first kind, $R^{(1)}_{nm}$ and $R^{(3)}_{nm}$ are the radial functions of the first and third kind.[21] The time-dependence of the potentials $\mathrm{e}^{-\mathrm{i}\omega t}$ is omitted for simplicity. The particle size parameter is defined by $\epsilon = kd/2$, with $k = 2\pi/\lambda$ being the wavenumber of the incident beam.

To solve the scattering problem, the beam-shape coefficient is known *a priori*. Where as the scattering coefficient is to be determined from the boundary conditions in the particle surface $\xi = \xi_0$. For for a rigid particle, one requires that the normal component of fluid velocity be zero on the particle surface, $\partial_\xi \left(\phi_{\text{in}} + \phi_{\text{sc}}\right)_{\xi=\xi_0} = 0$. Therefore, using the potentials in (3) we find

$$s_{nm} = -\frac{R^{(1)\,\prime}_{nm}(\epsilon, \xi_0)}{R^{(3)\,\prime}_{nm}(\epsilon, \xi_0)}, \tag{4}$$

with the prime symbol denoting differentiation with respect to ξ_0.

We limit our analysis to small particles compared to the wavelength, i.e. the so-called long-wavelength limit, which implies $\epsilon \ll 1$. In this approximation, only the monopole $n = 0$ and dipole $n = 1$ are relevant in the scattered wave description[22]. After substituting the spheroidal radial functions given in Eqs. (10) and (18) of Ref. 23 into Eq. (4), we Taylor-

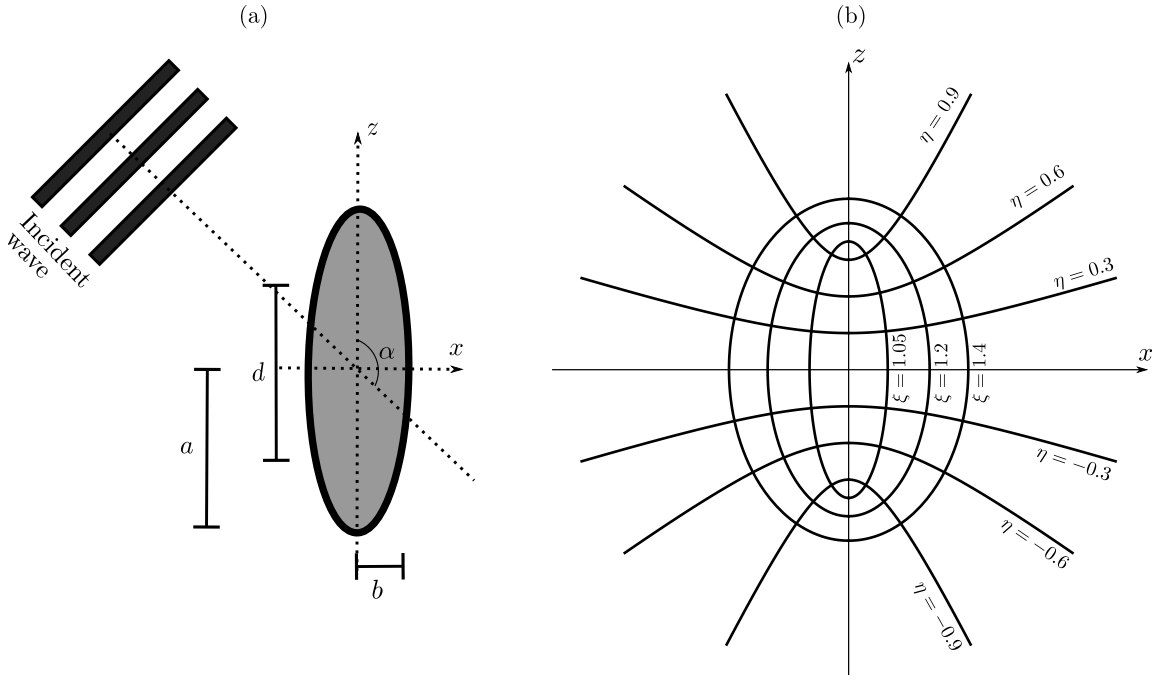

Fig. 1. (a) An arbitrary incident wave is scattered by a prolate spheroidal particle with major and minor axis denoted, respectively, by $2a$ and $2b$, and interfocal distance d. The wave incidence angle is denoted by α. (b) A system of prolate spheroidal coordinates with $d = 1$ and rotational symmetry around the z-axis.

81 expand the result around $\epsilon = 0$ to obtain the scattering coefficients,

$$s_{00} = -\frac{\mathrm{i}\epsilon^3}{3} f_{00} - \frac{\epsilon^6}{9} f_{00}^2, \quad s_{10} = \frac{\mathrm{i}\epsilon^3}{6} f_{10} - \frac{\epsilon^6}{36} f_{10}^2, \quad s_{1,-1} = s_{11} = \frac{\mathrm{i}\epsilon^3}{12} f_{11} - \frac{\epsilon^6}{144} f_{11}^2. \tag{5}$$

The scattering factors are expressed by

$$f_{00} = \xi_0 \left(\xi_0^2 - 1\right) = \frac{3k^3 V}{4\pi\epsilon^3}, \quad f_{10} = \frac{2}{3}\left[\frac{\xi_0}{\xi_0^2 - 1} - \ln\left(\frac{\xi_0 + 1}{\sqrt{\xi_0^2 - 1}}\right)\right]^{-1},$$
$$f_{11} = \frac{8}{3}\left[\frac{2 - \xi_0^2}{\xi_0\left(\xi_0^2 - 1\right)} + \ln\left(\frac{\xi_0 + 1}{\sqrt{\xi_0^2 - 1}}\right)\right]^{-1}, \tag{6}$$

where V is the particle volume.

In the farfield $\xi \to \infty$, we find from (2) that the spheroidal system reduces to the spherical coordinate $\epsilon\xi = kr + \mathrm{O}(\xi^{-1})$, $\eta = \cos\theta + \mathrm{O}(\xi^{-2})$, where r and θ are spherical coordinates. Moreover, the spheroidal functions become[21]

$$R_{nm}^{(1)}(\epsilon,\xi) \underset{\epsilon\xi\to\infty}{\sim} \frac{1}{kr}\sin\left(kr-\frac{n\pi}{2}\right), \quad R_{nm}^{(3)}(\epsilon,\xi) \underset{\epsilon\xi\to\infty}{\sim} \mathrm{i}^{-n-1}\frac{\mathrm{e}^{\mathrm{i}kr}}{kr}, \quad S_{nm}(\epsilon,\eta) \underset{\epsilon\to 0}{\sim} P_n^m(\cos\theta), \tag{7}$$

with P_n^m being the associated Legendre polynomial.

It is useful to introduce the spherical harmonics as

$$Y_n^m(\theta,\varphi) = \sqrt{\frac{2n+1}{4\pi}\frac{(n-m)!}{(n+m)!}}P_n^m(\cos\theta)\mathrm{e}^{\mathrm{i}m\varphi}. \tag{8}$$

After substituting (7) into (3) and using Eq. (8), we obtain the incident and scattered velocity potentials in the farfield $kr \gg 1$ as

$$\psi_{\mathrm{in}} = \frac{1}{kr}\sum_{n,m}\tilde{a}_{nm}\sin\left(kr-\frac{n\pi}{2}\right)Y_n^m(\theta,\varphi), \tag{9a}$$

$$\psi_{\mathrm{sc}} = \frac{\mathrm{e}^{\mathrm{i}kr}}{kr}\sum_{n=0}^{1}\sum_{m=-n}^{n}\mathrm{i}^{-n-1}\tilde{a}_{nm}s_{nm}Y_n^m(\theta,\varphi). \tag{9b}$$

Here, the potential functions are normalized to ϕ_0. Besides, the beam-shape coefficient in the spherical function basis is

$$\tilde{a}_{nm} = \sqrt{\frac{4\pi}{2n+1}\frac{(n+m)!}{(n-m)!}}a_{nm}. \tag{10}$$

Importantly, the coefficient $\tilde{a}_{nm}$ has been derived for different types of acoustic beams such as a traveling plane wave, Bessel vortex, Gaussian, and Bessel-Gaussian beam.[24] Numer-

ical schemes can also be used to compute the beam-shape coefficients of off-axial Bessel beams.[25–27]

The spheroidal wave functions asymptotically match the spherical wave functions in the farfield: $\phi_{\rm in} \to \psi_{\rm in}$ and $\phi_{\rm sc} \to \psi_{\rm sc}$, as $\epsilon\xi \to kr \to \infty$. We shall discuss next the use the farfield wavefunctions given in (9) to derive the acoustic radiation force acting on the spheroidal particle.

3. Acoustic radiation force

The acoustic radiation force exerted on an object is related to the net linear momentum removed from the incident beam by absorption and scattering processes.[28] Due to the conservation of linear momentum, we can obtain the radiation force by integrating the radiation stress tensor over a control spherical surface in the farfield centered at the particle. Taking this approach, the acoustic radiation force exerted on a particle is given by[20]

$$\boldsymbol{F}_{\rm rad} = \frac{E_0}{k^2}\boldsymbol{Q}_{\rm rad}, \tag{11}$$

where $E_0 = \rho_0 k^2 \phi_0^2/2$ is the characteristic energy density of the wave. The radiation force efficiency is given in terms of the farfield wave functions by

$$\boldsymbol{Q}_{\rm rad} = -(kr)^2 {\rm Re} \int_0^{2\pi}\int_0^{\pi} \left[\psi_{\rm sc}^* \left(1 - \frac{\rm i}{k}\partial_r\right)\psi_{\rm in} + |\psi_{\rm sc}|^2\right] \boldsymbol{e}_r \sin\theta \,{\rm d}\theta \,{\rm d}\varphi. \tag{12}$$

where $\boldsymbol{e}_r = \sin\theta\cos\varphi\,\boldsymbol{e}_x + \sin\theta\sin\varphi\,\boldsymbol{e}_y + \cos\theta\,\boldsymbol{e}_z$ is the radial unit-vector, with $\boldsymbol{e}_x$, $\boldsymbol{e}_y$, and $\boldsymbol{e}_z$ being Cartesian unit-vectors. The Cartesian components of the efficiency $\boldsymbol{Q}_{\rm rad}$ are derived by replacing (9) into Eq. (12) and performing the angular integrations. Accordingly, we find

to the dipole approximation

$$Q_x + \mathrm{i}Q_y = \frac{\mathrm{i}}{2}\left[\sqrt{\frac{2}{3}}\left[(s_{00} + s_{11}^* + 2s_{00}s_{11}^*)\tilde{a}_{00}\tilde{a}_{11}^* + (s_{00}^* + s_{1,-1} + 2s_0^* s_{1,-1})\tilde{a}_{00}^*\tilde{a}_{1,-1}\right]\right.$$
$$\left. + \sum_{m=-1}^{1}\sqrt{\frac{(2+m)(3+m)}{15}}\left(s_{1,m}\tilde{a}_{1,m}\tilde{a}_{2,m+1}^* + s_{1,-m}^*\tilde{a}_{1,-m}^*\tilde{a}_{2,-m-1}\right)\right], \tag{13a}$$

$$Q_z = \mathrm{Im}\left[\frac{1}{\sqrt{3}}\left(s_{00} + s_{10}^* + 2s_{00}s_{10}^*\right)\tilde{a}_{00}\tilde{a}_{10}^* + \sum_{m=-1}^{1}\sqrt{\frac{(2-m)(2+m)}{15}}s_{1,m}\tilde{a}_{1,m}\tilde{a}_{2,m}^*\right]. \tag{13b}$$

These equations are valid for an acoustic beam of arbitrary shape granted that its beam-shape coefficient $\tilde{a}_{nm}$ is known. Also, there is no restriction in the spheroid spatial orientation regarding the beam propagation direction. Furthermore, the method is suitable for an spheroid of any material composition (rigid, void, fluid, or viscoelastic solid) to which the scattering coefficients s_{nm} are to be determined by appropriate boundary conditions across the particle surface $\xi = \xi_0$.

4. Some wave examples

4.1 Traveling plane wave

Consider an incident plane wave

$$\phi_{\mathrm{in}} = \phi_0 \mathrm{e}^{\mathrm{i}\boldsymbol{k}\cdot\boldsymbol{r}}, \tag{14}$$

where $\boldsymbol{k} = k\left(\sin\alpha\cos\beta\,\boldsymbol{e}_x + \sin\alpha\sin\beta\,\boldsymbol{e}_y + \cos\alpha\,\boldsymbol{e}_z\right)$ is the wavevector, with α and β being its polar and azimuthal angles. Note that α is also the wave incidence angle regarding the particle major axis–see Fig. 1. The beam-shape coefficient of the plane wave is given by[24]

$$\tilde{a}_{nm} = 4\pi\mathrm{i}^n Y_n^{m*}(\alpha,\beta). \tag{15}$$

Other expressions of the beam-shape coefficient are noted for a Bessel vortex beam,[26,29] Gaussian beam,[30] and off-axial Bessel beam.[31] By replacing the scattering coefficient given in (5) and Eq. (15) into the equations in (13), we obtain the efficiency components for a rigid spheroidal particle as

$$Q_x = Q_k \sin\alpha\cos\beta, \quad Q_y = Q_k \sin\alpha\sin\beta, \quad Q_z = Q_k\cos\alpha, \tag{16}$$

where

$$Q_k = \frac{4\pi\epsilon^6}{9}\left[f_{00}^2 + \left(f_{00}f_{10} + \frac{3f_{10}^2}{4}\right)\cos^2\alpha + \frac{1}{2}\left(f_{00}f_{11} + \frac{3f_{11}^2}{8}\right)\sin^2\alpha\right]. \tag{17}$$

is the radiation force efficiency along the wave propagation direction Referring to Eq. (11), we find that the radiation force varies with frequency to the forth power, $F_{\rm rad} \sim \omega^4$. This dependence arises due to the connection of the radiation force with the Rayleigh scattering power, which also varies with frequency to the forth power. Moreover, the radiation force on the spheroid has the same frequency dependence as that exerted on a spherical particle.[4]

For small eccentricity $\epsilon_0 \ll 1$ ($\xi_0 \gg 1$), this equation becomes

$$Q_k(\alpha) = Q_0\left[1 - \frac{1}{22}\varepsilon_0^2(1+3\cos 2\alpha) + \frac{31}{3080}\varepsilon_0^4\left(1 - \frac{627}{155}\cos 2\alpha\right)\right], \tag{18}$$

where $Q_0 = 11k^6V^2/16\pi$ is the radiation force efficiency of a rigid spherical particle. For a wave of lateral ($\alpha = 90^\circ$) and frontal ($\alpha = 0$), we have $Q_k(90^\circ) = 1+(1/11)\varepsilon_0^2+(391/7700)\varepsilon_0^4$ and $Q_k(0) = 1-(2/11)\varepsilon_0^2-(59/1925)\varepsilon_0^4$. Clearly, lateral incidence produces more radiation force on the particle, $Q_k(90^\circ) > Q_k(0)$. We recover the classical radiation force result on a rigid sphere[2] by setting $\varepsilon_0 = 0$ and $\alpha = 0$, which yields $Q_k = Q_0$. On the other hand, when

the particle is a very slender prolate spheroid, the efficiency Q_k becomes

$$Q_k(\alpha) \underset{\varepsilon_0 \to 1}{\sim} \frac{34 Q_0}{33} \left(1 - \frac{5}{17} \cos 2\alpha\right). \tag{19}$$

Hence, the largest relative deviation from the radiation force on spherical particle of the same volume as the spheroid are $|1 - Q_k(0)/Q_0| = 3/11$ (frontal incidence, $\alpha = 0$) and $|1 - Q_k(90°)/Q_0| = 1/3$ (lateral incidence, $\alpha = 90°$).

In Fig. 2.a, we plot the radiation force efficiency Q_k/Q_0 along the wave propagation direction versus the incidence angle α. We consider a particle of different eccentricities $\varepsilon_0 = 0, 0.55, 0.86$. The efficiency monotonically increases with the incidence angle. With $40° < \alpha < 50°$, the efficiencies becomes larger than that of a spherical particle. The approximate solution (dashed lines) becomes inaccurate as the eccentricity increases.

4.2 Standing plane wave

Consider a standing wave formed by the superposition of two counter-propagating plane waves as described by Eq. (14). The incident wave function is expressed by

$$\phi_{\text{in}} = \phi_0 \cos\left[\boldsymbol{k} \cdot (\boldsymbol{r} + \boldsymbol{r}_0)\right] = \frac{\phi_0}{2} \left[\mathrm{e}^{\mathrm{i}\boldsymbol{k}\cdot(\boldsymbol{r}+\boldsymbol{r}_0)} + \mathrm{e}^{-\mathrm{i}\boldsymbol{k}\cdot(\boldsymbol{r}+\boldsymbol{r}_0)}\right], \tag{20}$$

where $\boldsymbol{r}_0$ is the distance from the particle center to the nearest pressure antinode, which lies in the same direction as the wavevector, thus, $\boldsymbol{k} \cdot \boldsymbol{r}_0 = k r_0$. To establish the partial-wave expansion of the standing wave, we notice that the expansion for a traveling plane wave is given by

$$\mathrm{e}^{\mathrm{i}\boldsymbol{k}\cdot(\boldsymbol{r}+\boldsymbol{r}_0)} = 4\pi \mathrm{e}^{\mathrm{i}kr_0} \sum_{n,m} \mathrm{i}^n Y_n^{m*}(\alpha, \beta)\, j_n(kr) Y_n^m(\theta, \varphi). \tag{21}$$

By replacing Eq. (21) into Eq. (20) and using the relation $Y_n^{m*} = (-1)^m Y_n^{-m}$, the beam-shape coefficient of the standing wave reads

$$\tilde{a}_{nm} = 4\pi \cos\left(kr_0 + \frac{n\pi}{2}\right) Y_n^{m*}(\alpha, \beta). \tag{22}$$

Substituting this coefficient into the equations of (13) along with the scattering coefficients of (5) yields

$$Q_x = Q_k \sin\alpha \cos\beta, \quad Q_y = Q_k \sin\alpha \sin\beta, \quad Q_z = Q_k \cos\alpha, \tag{23}$$

where

$$Q_k = \frac{4\pi}{9}\epsilon^3 \sin 2kr_0 \left(\frac{2}{3}f_{00} + f_{10}\cos^2\alpha + \frac{1}{2}f_{11}\sin^2\alpha\right) \tag{24}$$

is the efficiency along the wavevector direction. Referring to Eq. (11), we note that the radiation force varies with frequency linearly, $F_{\text{rad}} \sim \omega$. Note that this dependence is the same as that for a spherical particle.[4] The particle will be trapped in a pressure node granted that the quantity in the parenthesis of Eq. (24) is positive. Besides being trapped, the spheroidal particle can be set to spin around the y-axis due to the acoustic radiation torque.[32–34]

When the particle eccentricity is small $\varepsilon_0 \ll 1$, we have

$$Q_k(\alpha) = Q_0\left[1 - \frac{3}{100}\varepsilon_0^2(1 + 3\cos 2\alpha) + \frac{3}{7000}\varepsilon_0^4(5 - 69\cos 2\alpha)\right], \tag{25}$$

where $Q_0 = (k^3V/5)\sin 2kr_0$ is the radiation force efficiency for a spherical particle. Importantly, when $\alpha = 0$ this expression turns to

$$Q_k = Q_0\left(1 - \frac{3}{25}\varepsilon_0^2 - \frac{24}{875}\varepsilon_0^4\right). \tag{26}$$

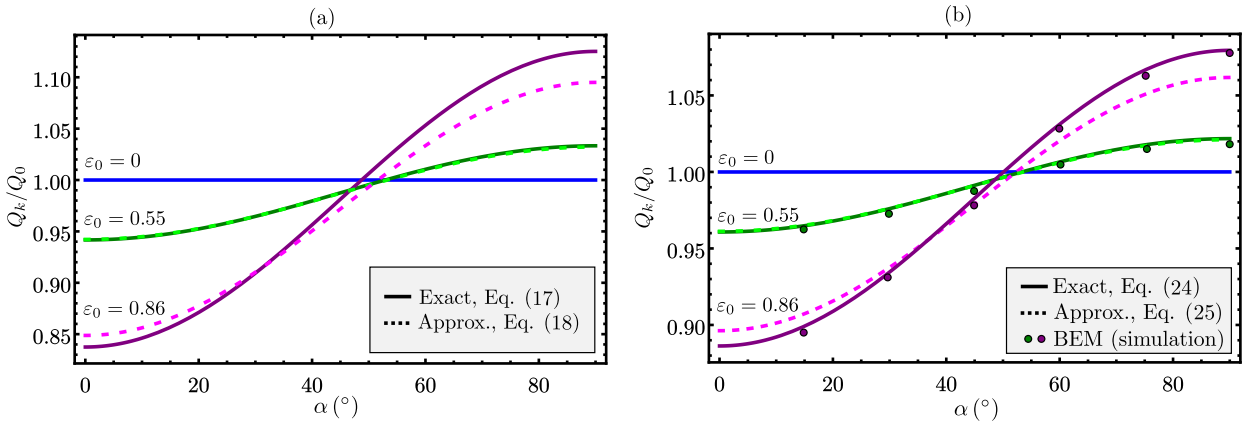

Fig. 2. Radiation force efficiency Q_k/Q_0 of a rigid prolate spheroid (with different eccentricities) caused by (a) a traveling and (b) standing plane wave versus the wave incidence angle α. Dots denote the numerical results obtained with the boundary-element method (BEM) as given in Ref. 19.

Writing this equation in terms of the aspect ratio $\varepsilon_1 = b/a - 1$, we find

$$Q_k = Q_0 \left(1 + \frac{6}{25}\varepsilon_1^2 + \frac{9}{875}\varepsilon_1^4\right). \tag{27}$$

This result was previously obtained by Marston *et al.*[14] When the eccentricity approaches one, the efficiency Q_k becomes

$$Q_k = Q_0 \left(1 - \frac{1}{5}\cos 2\alpha\right). \tag{28}$$

Therefore, the largest relative deviation from a spherical particle occurs $|1 - Q_k(0)/Q_0| = |1 - Q_k(90^\circ)/Q_0| = 1/5$, which correspond to the frontal and lateral incidence, respectively,

In Fig. 2.b, we present the radiation force efficiencies Q_k/Q_0 due to a standing plane wave as a function of the incidence angle α. The spheroidal particle has eccentricity $\varepsilon_0 = 0, 0.55, 0.86$. The efficiency increases with the incidence angle. The deviation of the spherical

particle case ($\varepsilon_0 = 0$) is more acute for high-eccentricity particles. Moreover, the approximate solution (dashed lines) given in Eq. (25) becomes inaccurate when $\varepsilon_0 > 0.8$. Excellent agreement is found between the exact solution and the boundary-element method as given in Ref. 19.

5. Summary and conclusions

We have calculated the acoustic radiation force exerted by an arbitrary wave on a spheroidal rigid particle in the long-wavelength limit. The general formulation gives the radiation force as a function of the scattering coefficients that represent the weight of each mode in the scattered waves. Exact results to the dipole approximation are presented for a rigid prolate spheroid considering a traveling and standing plane wave of arbitrary spatial orientation. Our results show that the largest relative deviation of the radiation force compared to the case of a spherical particle with the same volume as the spheroid are 1/3 (traveling plane wave) and 1/5 (standing plane wave). Approximate solutions of the radiation force are accurate for particles with eccentricity $\varepsilon_0 < 0.8$. Our analysis recovers previous theoretical results for a standing wave in the axisymmetric configuration.[14] Additionally, excellent agreement is found between the exact solution and the boundary-element method.[19]

The developed theoretical framework can be readily applied to spheroidal particles composed of fluid, elastic, and viscoelastic material, by solving the appropriate boundary conditions to find the scattering coefficients. Thermoviscous effects can also be accounted in the present theory. The method can also be promptly adapted to oblate spheroidal particles.

In conclusion, our work brings the theoretical analysis of the acoustic radiation force on small spheroidal particles to the same level as that for spherical particles. The obtained results further extend our knowledge on the underlying mechanisms of the radiation force phenomenon. Our findings are particularly useful for particle manipulation in acoustofluidic and acoustical tweezer techniques.

Acknowledgments

This work was supported by CNPq (National Research Council, Brazil), Grant No. 303783/2013-3 and 307221/2016-4, Royal Society (Newton Advanced Fellowship, UK), Grant No. NA160200.

References and links

[1]H. Bruus, J. Dual, J. Hawkes, M. Hill, T. Laurell, J. Nilsson, S. Radel, S. Sadhal, and M. Wiklund, "Forthcoming lab on a chip tutorial series on acoustofluidics: Acoustofluidics–exploiting ultrasonic standing wave forces and acoustic streaming in microfluidic systems for cell and particle manipulation," Lab. Chip **11**, 3579–3580 (2011).

[2]L. V. King, "On the acoustic radiation pressure on spheres," Proc. R. Soc. London, Ser. A **147**(861), 212–240 (1934).

[3]K. Yosioka and Y. Kawasima, "Acoustic radiation pressure on a compressible sphere," Acta Acust. united Ac. **5**, 167–173 (1955).

[4]L. P. Gor'kov, "On the forces acting on a small particle in an acoustical field in an ideal fluid," Sov. Phys. Dokl. **6**, 773 (1962).

[5]R. Löfstedt and S. Putterman, "Theory of long wavelength acoustic radiation pressure," J. Acoust. Soc. Am. **90**, 2027–2033 (1991).

[6]C. P. Lee and T. G. Wang, "Acoustic radiation force on a bubble," J. Acoust. Soc. Am. **93**, 1637–1640 (1993).

[7]H. Bruus, "Acoustofluidics 7: The acoustic radiation force on small particles," Lab. Chip (12), 1014–1021 (2012).

[8]O. A. Sapozhnikov and M. R. Bailey, "Radiation force of an arbitrary acoustic beam on an elastic sphere in a fluid," J. Acoust. Soc. Am. **133**, 661–676 (2013).

[9]G. T. Silva, "Acoustic radiation force and torque on an absorbing compressible particle in an inviscid fluid," J. Acoust. Soc. Am. **136**, 2405–2413 (2014).

[10]J. P. Leão-Neto and G. T. Silva, "Acoustic radiation force and torque exerted on a small viscoelastic particle in an ideal fluid," Ultrasonics **71**, 1 – 11 (2016).

[11]D. Baresch, J.-L. Thomas, and R. Marchiano, "Observation of a single-beam gradient force acoustical trap for elastic particles: Acoustical tweezers," Phys. Rev. Lett. **116**, 024301 (2016).

[12]J. P. Leão-Neto, J. H. Lopes, and G. T. Silva, "Core-shell particles that are unresponsive to acoustic radiation force," Phys. Rev. Applied **6**, 024025 (2016).

[13]G. T. Silva and H. Bruus, "Acoustic interaction forces between small particles in an ideal fluid," Phys. Rev. E **90**, 063007 (2014).

[14]P. L. Marston, W. Wei, and D. B. Thiessen, "Acoustic radiation force on elliptical cylinders and spheroidal objects in low frequency standing waves," AIP Conf. Proc. **838**, 495–499 (2006).

[15]T. B. A. Senior, "Low-frequency scattering," J. Acoust. Soc. Am. **53**, 742–747 (1973).

[16]F. Mitri, "Acoustic radiation force on oblate and prolate spheroids in Bessel beams," Wave Motion **57**, 231 – 238 (2015).

[17]P. Glynne-Jones, P. P. Mishra, R. J. Boltryk, and M. Hill, "Efficient finite element modeling of radiation forces on elastic particles of arbitrary size and geometry," J. Acoust. Soc. Am. **133**, 1885–1893 (2013).

[18]K.-M. Lim and S. S. Rahnama, "Calculation of acoustic radiation force and moment in microfluidic devices," Intl. J. Mod. Phys.: Conf. Series **34**, 1460380 (2014).

[19]F. B. Wijaya and K.-M. Lim, "Numerical calculation of acoustic radiation force and torque acting on rigid non-spherical particles," Acta Acust. united Ac. **101**, 531–542 (2015).

[20]G. T. Silva, "An expression for the radiation force exerted by an acoustic beam with arbitrary wavefront," J. Acoust. Soc. Am. **130**, 3541–3545 (2011).

[21]C. Flammer, *Spheroidal Wave Functions* (Dover Publications, Inc., Mineola, NY, 2005).

[22]A. D. Pierce, *Acoustics: An Introduction to Its Physical Principles and Applications* (Acoustical Society of America, Melville, NY, 1989).

[23]J. E. Burke, "Note on spheroidal wave functions," Stud. Appl. Math. **45**, 425–431 (1966).

[24]F. G. Mitri and G. T. Silva, "Generalization of the extended optical theorem for scalar arbitrary-shape acoustical beams in spherical coordinates," Phys. Rev. E. **90**, 053204 (2014).

[25]G. T. Silva, "Off-axis scattering of an ultrasound Bessel beam by a sphere," IEEE Trans. Ultrason. Ferroelectr. Freq. Control **58**, 298–304 (2011).

[26]F. G. Mitri and G. T. Silva, "Off-axial acoustic scattering of a high-order Bessel vortex beam by a rigid sphere," Wave Motion **48**(5), 392 – 400 (2011).

[27]G. T. Silva, J. H. Lopes, and F. G. Mitri, "Off-axial acoustic radiation force of repulsor and tractor Bessel beams on a sphere," IEEE Trans. Ultrason. Ferroelectr. Freq. Control **60**, 1207–1212 (2013).

[28]L. Zhang, "From acoustic radiation pressure to three-dimensional acoustic radiation forces," J. Acoust. Soc. Am. **144**, 443–447 (2018).

[29]L. Zhang and P. L. Marston, "Geometrical interpretation of negative radiation forces of acoustical Bessel beams on spheres," Phys. Rev. E **84**, 035601(R) (2011).

[30]X. Zhang and G. Zhang, "Acoustic radiation force of a Gaussian beam incident on spherical particles in water," Ultrasound Med. Biol. **38**, 2007–2017 (2012).

[31]Z. Gong, P. L. Marston, W. Li, and Y. Chai, "Multipole expansion of acoustical Bessel beams with arbitrary order and location," J. Acoust. Soc. Am. **141**, EL574–EL578 (2017).

[32]Z. Fan, D. Mei, K. Yang, and Z. Chen, "Acoustic radiation torque on an irregularly shaped scatterer in an arbitrary sound field," J. Acoust. Soc. Am. **124**, 2727–2732 (2008).

[33]L. Zhang and P. L. Marston, "Acoustic radiation torque and the conservation of angular momentum (L)," J. Acoust. Soc. Am. **129**, 1679–1680 (2011).

[34]G. T. Silva, T. P. Lobo, and F. G. Mitri, "Radiation torque produced by an arbitrary acoustic wave," Europhys. Lett. **97**, 54003 (2012).